Normal and abnormal thermalization indicators in a one-dimensional low-density Jaynes-Cummings Hubbard model with and without dipole-dipole interaction

Qing Li [1,2] Jin-Lou Ma [1] and Lei Tan [1,*]

[1] *Lanzhou Center for Theoretical Physics, Key Laboratory of Theoretical Physics of Gansu Province, Lanzhou University, Lanzhou, Gansu 730000, China*

[2] *School of Jia Yang, Zhejiang Shuren University, Shaoxing, Zhejiang 312028, China*

(Received 30 April 2022; accepted 16 November 2022; published 6 December 2022)

In the one-dimensional low-density Jaynes-Cummings Hubbard (JCH) model, we find that when the hopping strength is much smaller than the coupling strength, the average restricted energy gap ratio exhibits an abnormal statistical behavior that is neither a Poisson nor a Gaussian orthogonal ensemble. But the average half-chain entanglement entropy exhibits ergodicity, and the eigenstate thermalization hypothesis (ETH) is valid for the observable. These results are quite different from those of the standard JCH model. In addition, when the hopping and the coupling strengths are of the same order, quantum chaos still appears in the low-density JCH model, which is in contrast to the integrability of the one-dimensional hard-core bosons. Finally, the dipole-dipole interaction breaks the particle-hole symmetry and leads the abnormal statistical properties to be closer to those of the integrable system at the weak hopping strength limit, but the quantum chaos properties cannot be affected when the hopping strength is of the same order as the coupling strength. Our results demonstrate the counterintuitive behavior in the low-density JCH model and explain the physics behind them from the perspective of the energy spectrum.

DOI: 10.1103/PhysRevE.106.064107

I. INTRODUCTION

The important step in the understanding of quantum chaotic systems and integrable systems comes from the analysis of the distribution of the spacings between neighboring energy levels [1–4]. The quantum levels of integrable systems are not correlated and levels may cross, so the distribution is Poissonian [5–7] and the average of the restricted gap ratio is $\tilde{r}_{\text{poisson}} \approx 0.3863$ [8–10]. In quantum chaotic systems, crossings are avoided and the level spacing distribution is given by the Wigner-Dyson distribution [5,6,11,12], and the restricted gap ratios agree with predictions of the Gaussian orthogonal ensemble, $\tilde{r}_{\text{GOE}} \approx 0.5307$ [8,10,13].

Most quantum chaotic systems have been shown to be thermalized [14–18], and the necessary condition for thermalization is the eigenstate thermalization hypothesis (ETH) [19–21], which is numerically shown to be valid in quantum many-body systems [21–23]. For an observable, the matrix elements can be described by the ETH in the eigenstate of the general quantum Hamiltonian [24,25]. When the validity of the ETH is established, the diagonal matrix elements of the observables are smooth functions of energy. In other words, the eigenstate-to-eigenstate fluctuations decrease exponentially fast with increasing system size [22,23,26–29]. In addition, the off-diagonal matrix elements are exponentially small in the system size [14,26,30–32].

We discuss the above concerns in the standard JCH model [33–35] and have obtained some important conclusions. For the periodic boundary condition, the energy spectrum is massively degenerate in the JCH model with weak hopping strength. After removing the degenerate levels, the energy spectrum obeys the Poisson distribution, which proves that the system is nearly integrable, and the finite-size scalings of the diagonal and the off-diagonal matrix elements show that the ETH is invalid [36]. For the open boundary condition, we find that in the JCH model with the weak hopping strength, the energy spectrum meets the standard Poisson distribution and the average of the restricted gap ratio is close to 0.3863, which presents that the JCH model is not a quantum chaotic system and the ETH is invalid [37].

The coupling between the atom and the photon produces a photon blocking effect [33,38], where the presence of a single photon in a driven cavity prevents more photons from entering, which provides a reasonable approximation for the existence of a low-density JCH model. Second, the JC (Jaynes-Cummings) model can be solved analytically. When the weak hopping strength is introduced, the standard JCH model formed by coupling multiple JC models is a nearly integrable system [36], and the one-dimensional hard-core bosons are integrable [17,39,40], so we guess that the low-density JCH model is also integrable. To test this conjecture, we discuss whether the statistics of the energy spectrum and thermalization properties conform to the indicators of an integrable system in the low-density JCH model. In addition, we can calculate larger system sizes by the exact diagonalization in the low-density JCH model, which is helpful for us to observe finite-size scalings of the matrix elements.

The study of the low-density JCH model is only limited to the quantum phase transition. Supersolids are found in

*tanlei@lzu.edu.cn

the triangular lattice [41,42], and that model focuses on the single excitation rather than a single photon in each lattice site. In this paper we are concerned about the similarities and differences of the thermal properties in the low-density JCH model and the standard JCH model. In addition, since the dipole-dipole interaction between atoms can lead to the emergence of supersolids in the JCH model, we want to explore what interesting thermalization properties it will lead to in the low-density JCH model.

We first calculate the statistic of neighboring energy level spacings described by the averages of restricted gap ratios $\tilde{r}_{av}$, which exhibits an intermediate value between the Poisson and Gaussian orthogonal ensemble with the weak hopping limit $J/g = 0.01, 0.001$, and agrees with predictions of the Gaussian orthogonal ensemble in the case of $J/g = 1$ in the low-density JCH model. But in the low-density extended Jaynes-Cummings Hubbard (EJCH) model with weak hopping limit, $\tilde{r}_{av}$ is smaller than the intermediate value and has a strong dependence on system size. Through the half-chain entanglement entropy and its average, we find that the maximum value touches the Page value, and the slope is close to the Page value at $J/g = 0.01, 0.001$ in the low-density JCH model, but the results converge in the low-density EJCH model. Finally, we discuss matrix elements of observables and verify that the Hamiltonian eigenstates in the bulk of the spectrum obey ETH in the low-density JCH model with different parameters $J/g = 0.01, 0.001, 1$, but the ETH is invalid in the low-density EJCH model with parameters $J/g = 0.01, 0.001$.

The paper is organized as follows. We introduce the symmetry of the low-density JCH model and EJCH model in Sec. II. We study the average restricted energy gap ratio and the half-chain entanglement entropy in Sec. III. In Sec. IV we analyze thermalization properties and explore the relation between the symmetry and the distribution of matrix elements with a weak hopping strength limit. We verify the validity of the ETH when the hopping strength is of the same order of the coupling strength in Sec. V. We draw our conclusions in Sec. VI.

II. MODEL AND SYMMETRY

The Hamiltonian of a one-dimensional low-density JCH model is ($\hbar = 1$)

$$\hat{H}(t) = \sum_{j}^{M}[\omega_c \hat{a}_j^\dagger \hat{a}_j - J(\hat{a}_j^\dagger \hat{a}_{j+1} + \hat{a}_{j+1}^\dagger \hat{a}_j) + \varepsilon_0 \hat{\sigma}_j^+ \hat{\sigma}_j^- + g(\hat{a}_j \hat{\sigma}_j^+ + \hat{a}_j^\dagger \hat{\sigma}_j^-)], \tag{1}$$

where the first and third terms describe the free energies of photons and atoms on every site, $\hat{a}_j^\dagger(\hat{a}_j)$ is the creation (annihilation) operator of the photon, while $\hat{\sigma}_j^+ = |\mathrm{e}\rangle\langle\mathrm{g}|$ and $\hat{\sigma}_j^- = |\mathrm{g}\rangle\langle\mathrm{e}|$ are the spin-flip operators for atoms on site j. The parameters ω_c and ε_0 are the frequency of the cavity field and the transition frequency of the atom, respectively. The second term is the nearest-neighbor hopping of the photons, and the hopping strength is denoted by J. The last term is the coupling between photons and atoms in the same site with strength g. We define the total excitation number operator involved photons and atoms as $\hat{N} = \sum_{j=1}^{M} \hat{N}_j = \sum_{j=1}^{M}(\hat{a}_j^\dagger \hat{a}_j + \hat{\sigma}_j^+ \hat{\sigma}_j^-)$, and the total number of excitations $\langle \hat{N} \rangle$ is conservative, which equals the number of lattice sites M. Importantly, we mainly focus on the case that the JCH model is excited at low density $\rho \equiv \langle \hat{N} \rangle / M = 1$, where the maximum of photons is taken one in each cavity, so $(\hat{a}_j^\dagger)^2 = (\hat{a}_j)^2 = 0$.

In the resonant case ($\omega_c = \varepsilon_0$), using the operator $\hat{U} = \exp\{-i\sum_{j=1}^{M}(\omega_c \hat{a}_j^\dagger \hat{a}_j + \varepsilon \hat{\sigma}_j^+ \hat{\sigma}_j^-)\}t$, the Hamiltonian can be changed as follows in the rotating frame [37]:

$$\hat{H}_{\mathrm{JCH}} = g\sum_{j}^{M}(\hat{a}_j \hat{\sigma}_j^+ + \hat{a}_j^\dagger \hat{\sigma}_j^-) - J\sum_{j}^{M}(\hat{a}_j^\dagger \hat{a}_{j+1} + \hat{a}_{j+1}^\dagger \hat{a}_j). \tag{2}$$

For the standard JCH model, the Hamiltonian has reflection symmetry and chiral symmetry. The reflection symmetry makes extra degenerates in the energy spectrum, so it is necessary to calculate the statistics of the energy spectrum in the subspace of reflection symmetry. The chiral symmetry leads the energy spectrum to be symmetric around $E = 0$, and the diagonal elements also exhibit symmetry with the eigenvalue [37]. However, in the low-density JCH model, the system also has particle-hole symmetry, which not only leads to level crossings but also affects the distribution of the diagonal and off-diagonal elements for specific observables. After the particle-hole transformation $\hat{\mathcal{C}} = \prod_j^M (\hat{a}_j^\dagger + \hat{a}_j)\hat{\sigma}_j^x \hat{\kappa}$, the cavity field operator $\hat{a}$ and the two-level atomic operator $\hat{\sigma}^+$ become $\hat{a}^\dagger$ and $\hat{\sigma}^-$, respectively. $\hat{\kappa}$ is a complex conjugate operator to ensure that the particle-hole operator is antilinear [43]. For example, the particle-hole operator should satisfy $\hat{\mathcal{C}} i \hat{\mathcal{C}}^{-1} = -i$, and the particle-hole symmetry of the Hamiltonian $\hat{H}$ is verified by $\hat{\mathcal{C}}\hat{H}\hat{\mathcal{C}}^{-1} = \prod_j^M (\hat{a}_j^\dagger + \hat{a}_j)\hat{\sigma}_j^x \hat{H}^* \prod_j^M \hat{\sigma}_j^x (\hat{a}_j^\dagger + \hat{a}_j) = \hat{H}$. In addition, the photon operators satisfy an anticommutation relationship $\{\hat{a}_i, \hat{a}_i^\dagger\} = 1$ instead of a commutation relationship $[\hat{a}_i, \hat{a}_i^\dagger] = 1$ in the same site. At different sites, the photons obey $[\hat{a}_i, \hat{a}_j^\dagger] = [\hat{a}_i, \hat{a}_j] = [\hat{a}_i^\dagger, \hat{a}_j^\dagger] = 0$. This is an interesting system, and as we will see later, this anticommutation relationship has a pronounced impact on the distribution of the different observables.

In the low-density JCH model we introduce the dipole-dipole interaction between atoms and discuss the symmetry and thermalization properties. The Hamiltonian of the extended low-density JCH model is defined as

$$\hat{H}_{\mathrm{EJCH}} = \hat{H}_{\mathrm{JCH}} + V\sum_{j}^{M} \hat{n}_j^\sigma \hat{n}_{j+1}^\sigma, \tag{3}$$

where $\hat{n}_j^\sigma = \sigma_j^+ \sigma_j^-$ is the number of excitations of the atomic levels at lattice site j, and V denotes the dipole-dipole interaction strength, which breaks the particle-hole symmetry. After the particle-hole transformation, the dipole-dipole interaction term becomes $V\sum_j^M (\hat{n}_j^\sigma - \hat{\sigma}_j^z)(\hat{n}_{j+1}^\sigma - \hat{\sigma}_{j+1}^z)$, which breaks the invariance of the Hamiltonian.

Once the open boundary condition is applied, the Hamiltonians $\hat{H}_{\mathrm{JCH}}$ and $\hat{H}_{\mathrm{EJCH}}$ commute with the total excitation number $\hat{N}$, i.e., $[\hat{H}_{\mathrm{JCH}}, \hat{N}] = [\hat{H}_{\mathrm{EJCH}}, \hat{N}] = 0$, so they are U(1) symmetric. But we focus on reflection symmetry and particle-hole symmetry, because the distribution of the energy spectrum depends on their properties. Using the exact diagonalization, the largest lattice site is $M = N = 9$, whose

Hamiltonian matrix has dimension $D = \sum_{s=0}^{N} (\frac{N!}{s!(N-s)!})^2 = 48\,620$, and the dimension of the subspace with symmetries is $D_{\text{odd}} \approx D/4$.

III. SPECTRAL STATISTICS AND HALF-CHAIN ENTANGLEMENT ENTROPY

In Eq. (2) it can be seen that when the coupling strength $g = 0$, only the hopping term of the photon remains in the Hamiltonian, which is similar to hard-core bosons on a one-dimensional lattice. When the hopping strength $J = 0$, the Hamiltonian reduces to the JC model, which is solvable. But here we focus on the systems where the coupling strength and the hopping strength are not equal to zero. In the following discussion, reduced hopping strength and the reduced dipole-dipole interaction strength are obtained by dividing by the coupling strength.

The average of the statistics of the restricted gap ratio is an important indicator to characterize the integrability and chaos. The restricted gap ratio is defined as [8]

$$\tilde{r}_\alpha = \frac{\min\{E_{\alpha+1} - E_\alpha, E_\alpha - E_{\alpha-1}\}}{\max\{E_{\alpha+1} - E_\alpha, E_\alpha - E_{\alpha-1}\}}, \tag{4}$$

where E_α is the eigenvalue ordered in increasing values of energy. We study the average of $\tilde{r}_\alpha$ over the range of η $\tilde{r}_{av} = \langle \tilde{r} \rangle_\eta$. η satisfies the inequalities as follows:

$$\frac{E_{av} - E_\alpha}{E_{av} - E_{\min}} < \eta \quad \text{if} \quad E_\alpha < E_{av} \tag{5}$$

and

$$\frac{E_\alpha - E_{av}}{E_{\max} - E_{av}} < \eta \quad \text{if} \quad E_\alpha > E_{av}, \tag{6}$$

where $E_{av} = \langle \hat{H} \rangle = D^{-1} Tr\{\hat{H}\}$ is the average energy of the system. We have proved that different values of η have little effect on the spread of the eigenstate-to-eigenstate fluctuations of the observable with increasing system size [37], so we choose $\eta = 1/3$. In Figs. 1(a) and 1(b), we show the average restricted energy gap ratio $\tilde{r}_{av}$ in Eqs. (2) and (3) as a function of the reduced hopping strength J/g. Here we discuss two cases by tuning the parameters of the Hamiltonian. First, when the hopping strength is much smaller than the coupling strength ($J/g \ll 1$), the average restricted energy gap ratio converges to $\tilde{r}_{av} \approx 0.42$ in the low-density JCH system from Fig. 1(a). This shows that this abnormal statistical behavior is neither a Poisson nor the Gaussian orthogonal ensemble but an intermediate distribution independent of the finite-size effects. From Fig. 1(b) it can be seen that $\tilde{r}_{av}$ is lower than 0.42 for different system sizes, which means that the dipole-dipole interaction leads the intermediate distribution to be close to the Poisson distribution. In addition, the average restricted energy gap ratio increases with increasing system size, which has a strong dependence on the system size. Second, when the hopping strength and the coupling strength are of the same order, $\tilde{r}_{av}$ is distributed near 0.5307 and the system shows stable chaotic behavior, which is less dependent on the system size. In addition, when the dipole-dipole interaction is considered, the parameter range where quantum chaos emerges is enlarged, which is more pronounced at small system sizes.

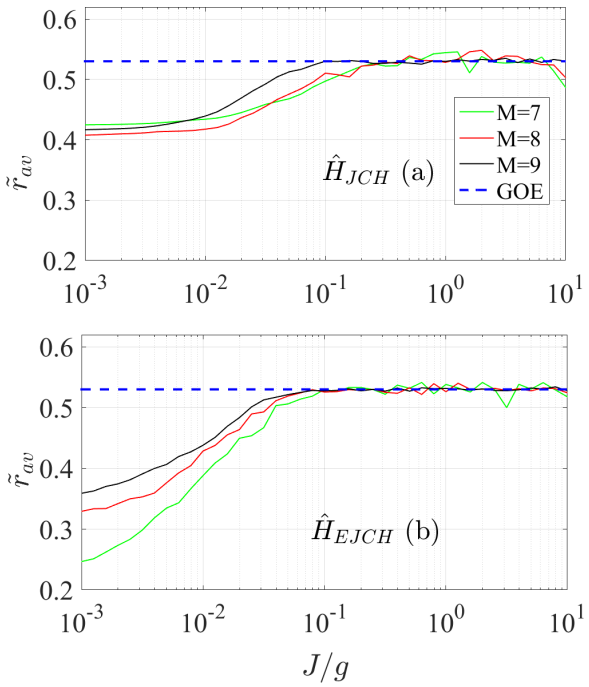

FIG. 1. The average restricted energy gap ratio $\tilde{r}_{av}$ as a function of the reduced hopping strength J/g in different system sizes. The dashed line represents $\tilde{r}_{\text{GOE}} \approx 0.5307$. The low-density JCH system is shown on the top, and the low-density EJCH system with a reduced interaction strength between atoms $V/g = 0.5$ is shown on the bottom.

In ergodic systems, the eigenstate thermalization hypothesis is proved to be valid, which is the mechanism of system thermalization [14,44], where the eigenstates of the Hamiltonian are fully random strongly entangled states (Page value) [45]. Therefore the average half-chain entanglement entropy has a volume law and exhibits the characteristics of rapidly reaching saturation in time [46–48]. Conversely, in a non-ergodic system, the eigenstates are weakly entangled states, and the average half-chain entanglement entropy obeys an area law with the system size, which exhibits a $\log(t)$ scaling behavior in time [46,49–53].

Next, we discuss the entanglement entropy of the system. The eigenvalue of the Hamiltonian is defined as E_α, and its corresponding eigenstate is $|\alpha\rangle$. It is convenient to compare the behavior of different system sizes using reduced eigenvalues $\varepsilon_\alpha = [E_\alpha - \min(E_\alpha)]/[\max(E_\alpha) - \min(E_\alpha)]$. Consider an important quantity with basis vectors independent, the half-chain entanglement entropy, which is defined in the following way. First, dividing the system into two subsystems A and B, when the number of lattice sites is even, the length of both the chains A and B takes $M/2$. When the number of lattice sites is odd, one takes $M/2 - 1$ and the other takes $M/2 + 1$. So the total Hilbert space is the tensor product $D(M) = D_A \bigotimes D_B$, and D_A and D_B are the dimensions of the Hilbert space of the subsystems A and B. Then the reduced density matrix for A is $\hat{\rho}_A^\alpha = \text{Tr}_B[|\alpha\rangle\langle\alpha|]$, where Tr_B is the partial trace over D_B. Thus the half-chain entanglement entropy is defined to be

$$\hat{S}_{M/2}^\alpha = -\text{Tr}_A\left[\hat{\rho}_A^\alpha \ln \hat{\rho}_A^\alpha\right]. \tag{7}$$

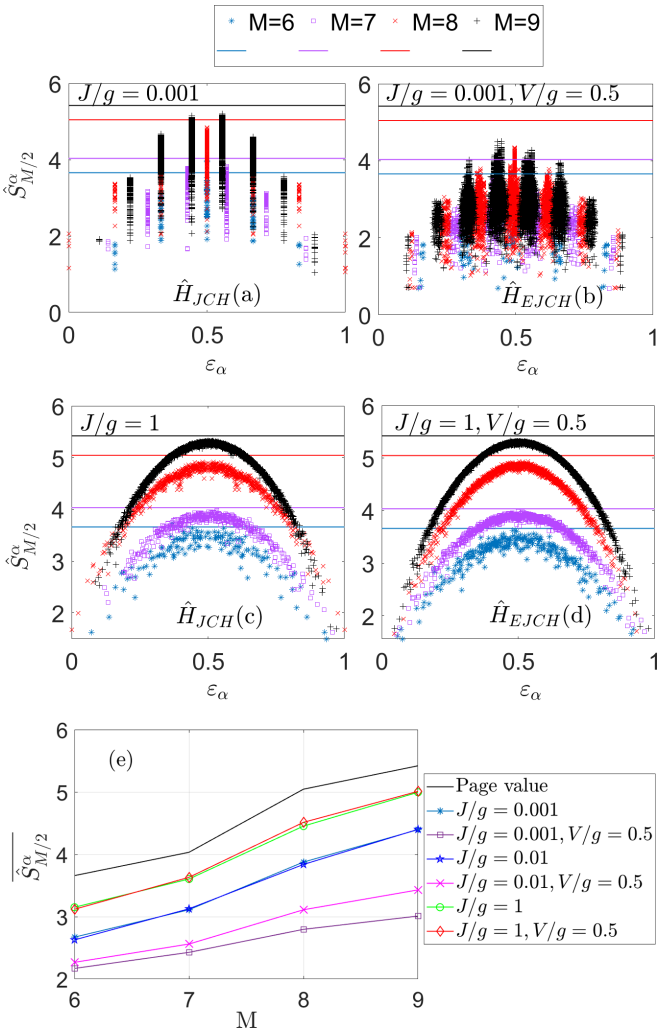

FIG. 2. (a)–(d) Change of the entanglement entropy between A and B with the reduced eigenvalue ε_α. The top of each figure shows different hopping strengths J/g and dipole-dipole interaction V/g. The horizontal lines are the Page value for different system sizes M. (e) Average of the entanglement entropy as a function of system size M.

For fully random states or the ergodic states, the mean von Neumann entanglement entropy is given by the Page value [45,54],

$$\overline{S_{\text{Page}}}(A) = \ln D_A - \frac{D_A}{2D_B}, \tag{8}$$

where the horizontal line represents the random vector average. We discuss the half-chain entanglement entropy $\hat{S}^{\alpha}_{M/2}$ and the corresponding Page value as a function of the reduced eigenvalue in three cases of the parameter $J/g = 0.001, 0.01, 1$. It can be seen from Fig. 2(a) that $\hat{S}^{\alpha}_{M/2}$ has an obvious structure, which is discontinuous with the change of reduced eigenvalues, but its maximum value is very close to the Page value. When the dipole-dipole interaction is considered, $\hat{S}^{\alpha}_{M/2}$ cannot touch the Page value for all system sizes in Fig. 2(b), which means that the low-density EJCH system does not conform to the properties of quantum chaos at $J/g = 0.001$. These results are similar to the case where the hopping strength is $J/g = 0.01$. When the hopping strength becomes of the same order of the coupling strength, Figs. 2(c) and 2(d) show that the dipole-dipole interaction has little effect on $\hat{S}^{\alpha}_{M/2}$. In addition, compared with the weak hopping limit, $\hat{S}^{\alpha}_{M/2}$ changes continuously as a function of the reduced eigenvalue, and its maximum value completely coincides with the Page value, marking the setting-on of quantum chaos. We further study the average over the eigenstates of the entanglement entropy, and the scales with the system size M are shown in Fig. 2(e). At different values of J/g and V/g, the slope is different. In the ergodic cases ($J/g = 0.001, J/g = 0.01, J/g = 1$ and $J/g = 1, V/g = 0.5$), the slopes are very close to that of the fully random Page value. When the ergodicity is broken ($J/g = 0.01, V/g = 0.5$ and $J/g = 0.001, V/g = 0.5$), the slope is smaller than the Page value.

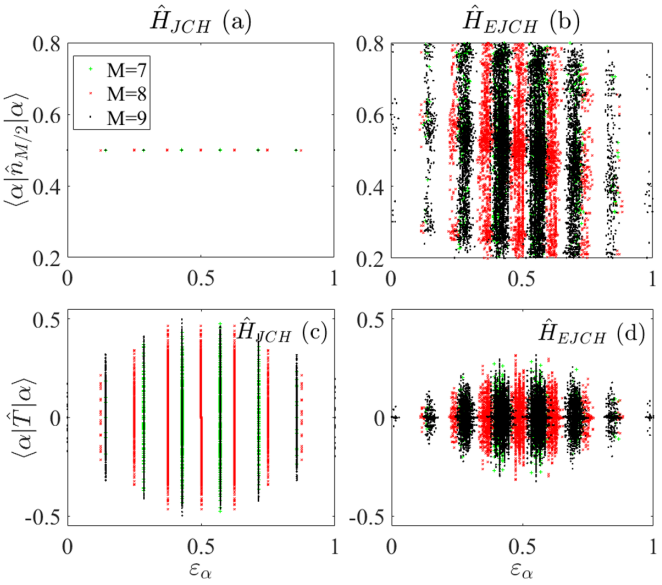

FIG. 3. The diagonal elements of observables $\langle\alpha|\hat{n}_{M/2}|\alpha\rangle$ and $\langle\alpha|\hat{T}|\alpha\rangle$ as a function of the reduced eigenvalues for different system sizes. The reduced hopping strength of photons is $J/g = 0.001$, and the reduced interaction strength is $V/g = 0.5$ in the low-density EJCH system. The graphical results are similar to the reduced hopping strength $J/g = 0.01$, and other parameters are invariant.

IV. THERMALIZATION PROPERTIES AT THE WEAK HOPPING LIMIT

In order to gain further insight into whether the low-density JCH system is close to integrability and chaos and the effect of the dipole-dipole interaction on the system at the weak hopping limit, we discuss the distribution of diagonal and off-diagonal matrix elements of the observables as a function of the system sizes to test the validity of the ETH in the low-density JCH and EJCH systems.

A. Diagonal matrix elements of observables

In the weak hopping limit, Figs. 3(a) and 3(c) show the diagonal elements of the occupation operator of photons in central site $\hat{n}_{M/2}$ and the kinetic energy operator of photons $\hat{T} = \frac{1}{M}\sum_j^M(\hat{a}_j^\dagger\hat{a}_{j+1} + \hat{a}_{j+1}^\dagger\hat{a}_j)$ in the low-density JCH system,

and different colors represent different system sizes. It can be seen from Fig. 3(a) that the diagonal matrix elements of $\hat{n}_{M/2}$ are equal to 0.5, and this behavior is independent of the system size. In addition, there is no fluctuation of the diagonal matrix elements, which is completely inconsistent with the distribution behavior of the standard JCH system [37]. Further, we find that the particle-hole symmetry in the low-density JCH model leads to the absence of fluctuations. When the system has particle-hole symmetry, the cavity field operator $\hat{a}$ becomes $\hat{a}^+$, and then the average value of the occupation operator of photons $\langle \hat{a}^+\hat{a}\rangle = \langle \hat{a}\hat{a}^+\rangle = 1 - \langle \hat{a}^+\hat{a}\rangle$, thus $\langle \hat{a}^+\hat{a}\rangle = 0.5$. However, in Fig. 3(c) the diagonal elements of the kinetic energy operator have large fluctuations which are not affected by the particle-hole symmetry. In Figs. 3(b) and 3(d), we discuss the distribution of the diagonal elements in the eigenstates of the low-density EJCH system for $\hat{n}_{M/2}$ and $\hat{T}$. It can be seen from Fig. 3(b) that when the dipole-dipole interaction is considered, the fluctuations of the diagonal elements for $\hat{n}_{M/2}$ are large for different system sizes, because the dipole-dipole interaction breaks particle-hole symmetry. Another interesting phenomenon is that the dipole-dipole interaction reduces the fluctuations of the diagonal elements of $\hat{T}$, which can be drawn from the comparison of Figs. 3(c) and 3(d). In addition, when the dipole-dipole interaction is considered, the variation of the diagonal elements of $\hat{T}$ with the reduced eigenvalues shifts from discontinuous to continuous. Therefore we believe that $\hat{n}_{M/2}$ is not suitable as an observable to discuss the validity of the ETH due to the particle-hole symmetry in the low-density JCH model, but it can still be used as an observable in the low-density EJCH model with the dipole-dipole interaction. Therefore, in the following discussion, we do not take the occupation operator of photons as an observable in the low-density JCH system.

In Fig. 3(c), the fluctuation of the diagonal matrix element of $\hat{T}$ is greatly large in the eigenstate of the low-density JCH system, and the fluctuation does not show a significant decrease with the increase of the system sizes. In order to make a more explicit relationship between fluctuation and system size, we calculate the eigenstate-to-eigenstate fluctuation of the diagonal matrix elements, which is given by

$$Z_\alpha(O) = \langle \alpha + 1|\widehat{O}|\alpha + 1\rangle - \langle \alpha|\widehat{O}|\alpha\rangle. \tag{9}$$

Within the energy window defined by η, the mean is defined as

$$\langle Z\rangle_\eta(O) = ||Z_\eta||^{-1} \sum_{|\alpha\rangle \in Z_\eta} |Z_\alpha(O)|, \tag{10}$$

where $||Z_\eta||$ is the number of corresponding eigenstates in Z_η.

Figure 4(a) shows the mean statistics of eigenstate-to-eigenstate fluctuations $\langle Z\rangle_\eta(\hat{n}_{M/2})$ in the low-density EJCH model with $J/g = 0.001$ and $V/g = 0.5$. The result shows that $\langle Z\rangle_\eta(\hat{n}_{M/2})$ does not decrease with increasing system size. Figure 4(b) presents the mean statistics of eigenstate-to-eigenstate fluctuations $\langle Z\rangle_\eta(\hat{T})$ as a function of system size in the low-density JCH system with $J/g = 0.01$ and $J/g = 0.001$. We can see that the dots are very close to the black line, implying that the scaling of the mean fluctuation is consistent with an exponential decrease with increasing system sizes. Therefore the diagonal part of the ETH is valid for the abnormal statistical behavior plotted at the weak hopping limit in Fig. 1(a). In addition, when the dipole-dipole interaction is considered, $\langle Z\rangle_\eta(\hat{T})$ deviates from the exponentially decreasing in Fig. 4(c), which leads to a violation of the ETH at the weak hopping limit in the low-density EJCH model.

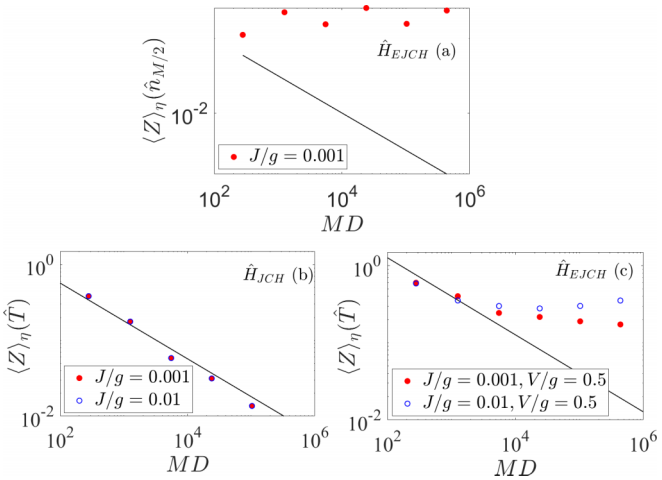

FIG. 4. Statistical mean of fluctuations of diagonal elements vs system size for same observables and model parameters as in Fig. 3. The black line as a reference exponentially decreases with size M. Here $\eta = 1/3$.

B. Off-diagonal matrix elements of observables

Next we discuss the distribution of the off-diagonal matrix elements of $\hat{T}$ to test the off-diagonal part of the ETH in the weak hopping limit. The discussions of the off-diagonal matrix elements are limited to a narrow energy window centered around the middle of the spectrum, which is defined by the following expression:

$$\left(1 - \frac{\epsilon}{2}\right) < \frac{\bar{\varepsilon}}{\varepsilon_{av}} < \left(1 + \frac{\epsilon}{2}\right). \tag{11}$$

Here ϵ is defined as the width of the window, $\bar{\varepsilon} = \frac{\varepsilon_\alpha + \varepsilon_\beta}{2}$, and ε_β is the reduced eigenvalue, where the corresponding eigenstate is $|\beta\rangle$.

Another reason why the occupancy operator cannot be used as an observable in the low-density JCH model is that the values of the off-diagonal elements for $\hat{n}_{M/2}$ are all zero, which is also caused due to the particle-hole symmetry. When the cavity field operator $\hat{a}$ becomes $\hat{a}^+$, the off-diagonal element $\langle \alpha|\hat{a}^+\hat{a}|\beta\rangle = \langle \alpha|\hat{a}\hat{a}^+|\beta\rangle = \langle \alpha|1 - \hat{a}^+\hat{a}|\beta\rangle = -\langle \alpha|\hat{a}^+\hat{a}|\beta\rangle$, and thus $\langle \alpha|\hat{a}^+\hat{a}|\beta\rangle = 0$.

Figures 5(a) and 5(b) show the off-diagonal matrix elements of $\hat{T}$ as a function of reduced eigenvalue difference ω. As ω increases, the off-diagonal elements tend to decrease and the distribution has obvious structure. This structure comes from the fact that the eigenvalues are divided, such as in Fig. 6(a). The eigenvalues are divided into many parts, and each part has a large number of quasidegenerate levels. When the dipole-dipole interaction is considered, we can see that the distribution is still structural, but there are more blocks of eigenvalues and some energy levels are repulsive. Therefore the dipole-dipole interaction has an influence on the distribution of the off-diagonal elements. Figures 5(c) and 5(d)

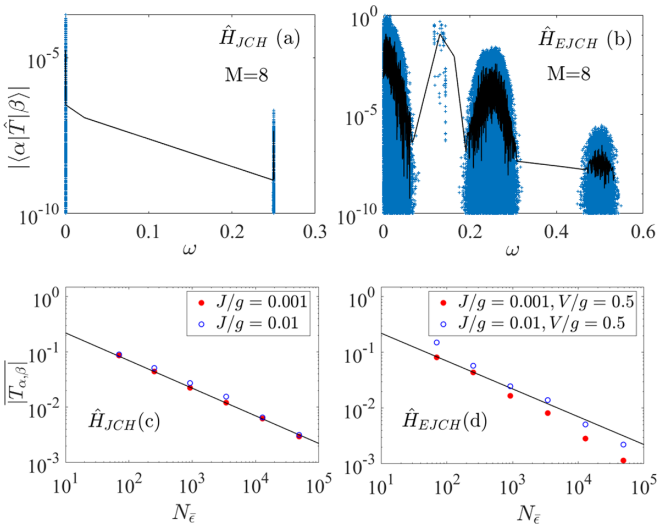

FIG. 5. (a, b) Absolute value of the off-diagonal matrix elements of the kinetic energy operator $|\langle\alpha|\hat{T}|\beta\rangle|$ vs the difference of the reduced eigenvalues $\omega = \varepsilon_\alpha - \varepsilon_\beta$. The eigenstates are chosen within the energy window of $\epsilon = 0.1$. The black lines are running averages with a subset length of 100. Other parameters have the same values as in Fig. 3. (c, d) Average of the absolute value of the off-diagonal matrix elements $\overline{|T_{\alpha,\beta}|}$ vs the number of eigenstates N_ϵ within a narrow energy window around ε_{av}, and solid lines are fit to $a(N_\epsilon)^{-0.5}$.

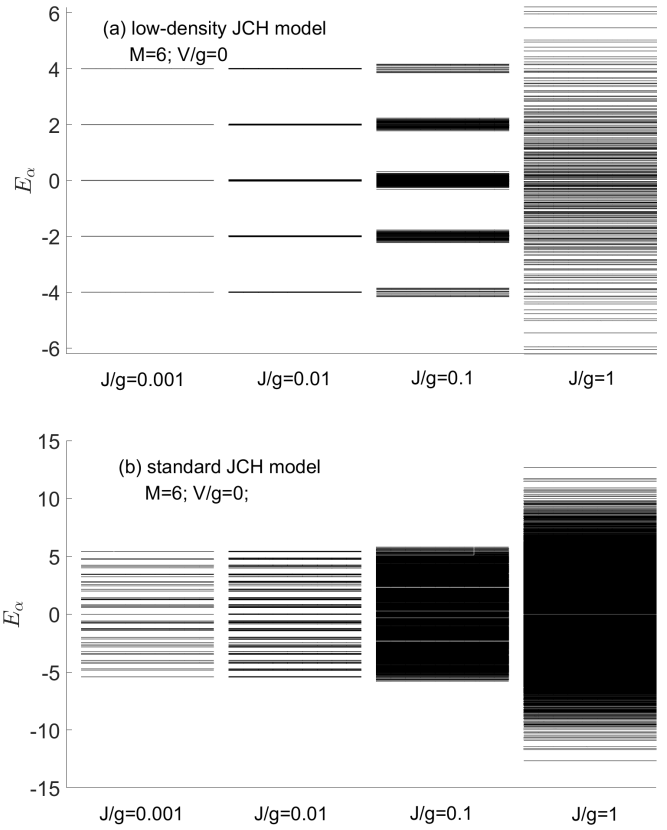

FIG. 6. The energy eigenvalues E_α for different reduced hopping strengths of the photon in the low-density JCH model (a) and standard JCH model (b). The selected sizes M of numerical calculation are $M = 6$.

describe the averages of the absolute value of the off-diagonal matrix elements $\overline{|T_{\alpha,\beta}|}$ as a function of the system sizes at the weak hopping limit ($J/g = 0.01$ and $J/g = 0.001$) in the low-density JCH and EJCH models. In the low-density JCH model, finite-size scalings of $\overline{|T_{\alpha,\beta}|}$ conform to the exponential decay, which satisfies the ETH. When adding the dipole-dipole interaction, $\overline{|T_{\alpha,\beta}|}$ does not satisfy exponential decay and violates the ETH in the low-density EJCH model.

Finite-size scalings of the diagonal and off-diagonal elements of the kinetic energy operator with system size in Figs. 4(b) and 5(c) show that the ETH is valid at the weak hopping limit in the low-density JCH model. This result is opposite to that of the standard JCH system under weak hopping. One explanation is that when there is no hopping term, the energy spectrum structure of the low-density JCH model is simple and the number of eigenstates is less compared to the standard JCH model, which is easily changed by perturbation. In the low-density JCH model, when the hopping term of photons in different cavities is not considered, the energy level distribution of this lattice chain is similar to that of the one-dimensional chain of harmonic oscillators, where all levels are equidistant. When the weak hopping strength of photons is added as a perturbation term compared to the original Hamiltonian, a single energy level is split into multiple energy levels, as shown in Fig. 6(a), and the repulsion between energy levels is stronger when the hopping strength is larger. Figure 6(b) shows the energy level distribution with different hopping strengths in the standard JCH model. We can see that they have common features, that is, the energy level is split and the energy level repulsion is stronger as the hopping strength increases. When the hopping term is not considered, both models are integrable and the energy spectrum can be solved analytically. However, as the hopping strength increases, the standard JCH model can become a nonintegrable model with a large hopping strength, and a small hopping strength is enough to generate a nonintegrable system in the low-density JCH model. We argue that when the hopping term is not considered, the low-density JCH model has fewer energy levels with a simple distribution and fewer eigenstates compared with the standard JCH model. Thus thermalization properties are more easily altered by the perturbed hopping term in the low-density JCH model.

V. EIGENSTATE THERMALIZATION AND QUANTUM CHAOS

In this section we demonstrate that the Hamiltonian eigenstates in the bulk of the spectrum obey the ETH in the low-density JCH system when the hopping strength is equal to the coupling strength ($J/g = 1$). Another purpose is to discuss how the dipole-dipole interaction affects the thermalization property of the system in this case.

In Figs. 7(a) and 7(b) the distributions of the diagonal matrix elements of the kinetic energy operator with eigenvalues are continuous and narrow. And the eigenstate-eigenstate fluctuations of the diagonal elements decrease exponentially with the increase of the system size from the subplots. Thus, in the low-density JCH and EJCH systems, the diagonal part of the ETH is valid. In addition, compared with the weak

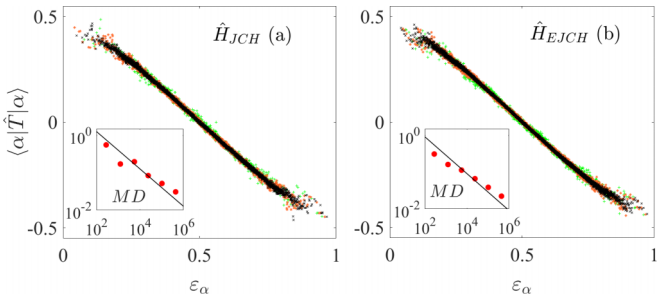

FIG. 7. $\langle\alpha|\hat{T}|\alpha\rangle$ as a function of the reduced energy for $J/g = 1$. Symbols represent results for $M = N = 7$ (green), $M = N = 8$ (red), and $M = N = 9$ (black). The subplots are the mean statistics of eigenstate-to-eigenstate fluctuations in Z_η vs MD. Solid lines are exponential decaying guides to the eyes.

hopping strength limit, the dipole-dipole interaction has little effect on the distribution of the diagonal matrix elements in the case of $J/g = 1$.

To further verify whether the off-diagonal part of the ETH holds in the low-density JCH and EJCH models with the case of $J/g = 1$, we introduce a ratio of off-diagonal elements, defined as [55]

$$\Gamma_{\hat{O}}(\omega) := \overline{|O_{\alpha\beta}|^2}/\overline{|O_{\alpha\beta}|}^2. \tag{12}$$

$\Gamma_{\hat{O}} = \pi/2$ corresponds to the matrix element of the normal distribution, $\overline{|O_{\alpha\beta}|^2}$ represents the coarse-grained average of $|O_{\alpha\beta}|^2$ over a small reduced ω window, and the width of the window is 0.05.

In Figs. 8(a) and 8(b) we show the ratios of the kinetic energy operator $\Gamma_{\hat{T}}$ in the low-density JCH and EJCH models, respectively. For most ω, $\Gamma_{\hat{T}}$ is indistinguishable from $\Gamma_{\hat{O}} = \pi/2$, indicating the distribution of off-diagonal elements is Gaussian. At large values of ω, $\Gamma_{\hat{T}}$ deviates from $\pi/2$. Furthermore, in Fig. 8(a) the dependence of $\Gamma_{\hat{T}}$ on the system size is more obvious, which can be obtained by comparing the green circle and the black star, but the fluctuations of the distribution decrease as the system size increases. When the dipole-dipole interaction is considered, the results are slightly different. From Fig. 8(b), for small ω, $\Gamma_{\hat{T}}$ has no dependence on small system size, and when ω increases, the size effect becomes obvious. However, as a whole, $\Gamma_{\hat{T}}$ can be described by a normal distribution. Therefore, from the above results we can conclude that in the case of the parameter $J/g = 1$, the

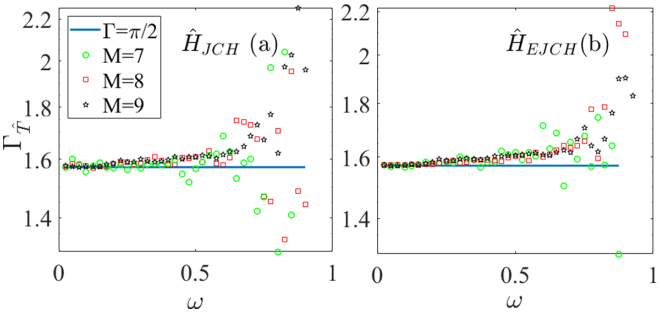

FIG. 8. The ratio of off-diagonal elements $\Gamma_{\hat{T}}$ vs the difference of the reduced eigenvalues. The blue line represents $\Gamma_{\hat{O}} = \pi/2$.

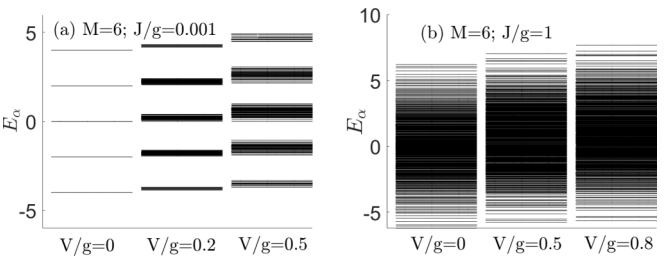

FIG. 9. The energy eigenvalues E_α for different reduced hopping strengths $J/g = 0.001$ (a) and $J/g = 1$ (b) in the low-density JCH model. The selected sizes M of numerical calculation are $M = 6$.

low-density JCH and EJCH systems are in good agreement with the ETH.

From the standpoint of the energy spectrum, we can see that the dipole-dipole interaction has a large influence on the low-density JCH system in the weak hopping limit ($J/g = 0.01, 0.001$), while it has a small influence in the same order of magnitude ($J/g = 1$). As shown in Fig. 9, there are different hopping strengths of the photon and dipole-dipole interaction strengths between atoms. From Fig. 9(a) we can see that in the weak hopping limit without the dipole-dipole interaction term, the energy spectrum is divided into blocks in the low-density JCH model, and there are many energy levels close to each other in each block. When small dipole-dipole interaction strength is considered, energy levels are rejected, and when large dipole-dipole interaction strength is considered, the repulsion between the energy levels becomes obvious. However, when the hopping strength is of the same order of the coupling strength, as shown in Fig. 9(b), the changes in the energy spectrum are small despite the dipole-dipole interaction strength is large. Therefore the dipole-dipole interaction can easily change the energy spectrum distribution of the low-density JCH model at the weak hopping limit, while it has little effect on the system energy spectrum when the hopping strength increases.

VI. CONCLUSION

When the open boundary condition is applied, the low-density JCH system has U(1) symmetry, chiral symmetry, reflection symmetry, and particle-hole symmetry. When a dipole-dipole interaction is considered, the particle-hole symmetry is broken. From an energy spectrum perspective, we find that the average restricted energy gap ratios converge to 0.42 in the low-density JCH system with the weak hopping limit for the finite size, which is not a Poisson or a Gaussian orthogonal ensemble. The dipole-dipole interaction leads the system to exhibit closer integrable behavior in the weak hopping limit. When the hopping strength is of the same order of the coupling strength, the average restricted energy gap ratio is close to 0.53 whether the dipole-dipole interaction is applied or not, which shows stable ergodicity. Next, from the perspective of eigenstates, we analyze that the half-chain entanglement entropy appears structurally distributed but the maximum value and the slope are very close to the Page value at the weak hopping limit, which implies that the low-density JCH system is ergodic. When the dipole-dipole interaction

is considered, the maximum value of the half-chain entanglement entropy cannot touch the Page value in all system sizes and the slope is smaller than the Page value; thus the low-density EJCH system is more inclined to be integrable at the weak hopping limit.

We focus on the distribution of the matrix elements of the occupation operator and the kinetic energy operator to test the validity of the ETH. In the low-density JCH model, the diagonal element distribution of the occupation operator has no fluctuation and the off-diagonal elements are all equal to zero due to the particle-hole symmetry, which is not suitable as an observable to test the validity of ETH. In addition, in the weak hopping limit, finite-size scalings of the diagonal and off-diagonal elements for the kinetic energy operator show that the ETH is valid in the low-density JCH system, while the dipole-dipole interactions destroy the validity of the ETH. When the hopping strength is equal to the coupling strength, the systems obey ETH whether the dipole-dipole interaction is considered or not. Our results provide a clear understanding of the thermalization properties in the low-density JCH model that cannot be inferred analogously from the standard JCH model.

ACKNOWLEDGMENTS

This work was supported by National Natural Science Foundation of China (Grants No. 11874190, No. 61835013 and No. 12047501). Support was also provided by the Supercomputing Center of Lanzhou University.

[1] F. J. Dyson, J. Math. Phys. **3**, 140 (1962).
[2] M. V. Berry and M. Tabor, Proc. R. Soc. London, Ser. A **356**, 375 (1977).
[3] O. Bohigas, M. J. Giannoni, and C. Schmit, Phys. Rev. Lett. **52**, 1 (1984).
[4] A. Gubin and L. F. Santos, Am. J. Phys. **80**, 246 (2012).
[5] F. Haake, *Quantum Coherence in Mesoscopic Systems* (Springer, New York, 1991), pp. 583–595.
[6] L. E. Reichl, *Transition to Chaos* (Springer, New York, 2004).
[7] T. Guhr, A. Müller-Groeling, and H. A. Weidenmüller, Phys. Rep. **299**, 189 (1998).
[8] V. Oganesyan and D. A. Huse, Phys. Rev. B **75**, 155111 (2007).
[9] S. Iyer, V. Oganesyan, G. Refael, and D. A. Huse, Phys. Rev. B **87**, 134202 (2013).
[10] O. Giraud, N. Macé, E. Vernier, and F. Alet, Phys. Rev. X **12**, 011006 (2022).
[11] R. V. Jensen, Nature (London) **355**, 311 (1992).
[12] H.-J. Stöckmann, *Quantum Chaos: An Introduction* (Cambridge University Press, Cambridge, England, 2000).
[13] Y. Y. Atas, E. Bogomolny, O. Giraud, and G. Roux, Phys. Rev. Lett. **110**, 084101 (2013).
[14] L. D'Alessio, Y. Kafri, A. Polkovnikov, and M. Rigol, Adv. Phys. **65**, 239 (2016).
[15] J. M. Deutsch, Rep. Prog. Phys. **81**, 082001 (2018).
[16] M. Rigol and M. Srednicki, Phys. Rev. Lett. **108**, 110601 (2012).
[17] L. F. Santos, A. Polkovnikov, and M. Rigol, Phys. Rev. Lett. **107**, 040601 (2011).
[18] K. Mallayya and M. Rigol, Phys. Rev. Lett. **120**, 070603 (2018).
[19] J. M. Deutsch, Phys. Rev. A **43**, 2046 (1991).
[20] M. Srednicki, Phys. Rev. E **50**, 888 (1994).
[21] M. Rigol, V. Dunjko, and M. Olshanii, Nature (London) **452**, 854 (2008).
[22] T. Yoshizawa, E. Iyoda, and T. Sagawa, Phys. Rev. Lett. **120**, 200604 (2018).
[23] H. Kim, T. N. Ikeda, and D. A. Huse, Phys. Rev. E **90**, 052105 (2014).
[24] M. Srednicki and F. Stiernelof, J. Phys. A: Math. Gen. **29**, 5817 (1996).
[25] M. Srednicki, J. Phys. A: Math. Gen. **32**, 1163 (1999).
[26] D. Jansen, J. Stolpp, L. Vidmar, and F. Heidrich-Meisner, Phys. Rev. B **99**, 155130 (2019).
[27] R. Mondaini, K. R. Fratus, M. Srednicki, and M. Rigol, Phys. Rev. E **93**, 032104 (2016).
[28] R. Steinigeweg, J. Herbrych, and P. Prelovšek, Phys. Rev. E **87**, 012118 (2013).
[29] W. Beugeling, R. Moessner, and M. Haque, Phys. Rev. E **89**, 042112 (2014).
[30] E. Khatami, G. Pupillo, M. Srednicki, and M. Rigol, Phys. Rev. Lett. **111**, 050403 (2013).
[31] W. Beugeling, R. Moessner, and M. Haque, Phys. Rev. E **91**, 012144 (2015).
[32] R. Mondaini and M. Rigol, Phys. Rev. E **96**, 012157 (2017).
[33] A. D. Greentree, C. Tahan, J. H. Cole, and L. C. Hollenberg, Nat. Phys. **2**, 856 (2006).
[34] M. J. Hartmann, F. G. Brandao, and M. B. Plenio, Nat. Phys. **2**, 849 (2006).
[35] D. G. Angelakis, M. F. Santos, and S. Bose, Phys. Rev. A **76**, 031805(R) (2007).
[36] Q. Li, J.-L. Ma, T. Huang, L. Tan, H.-Q. Gu, and W.-M. Liu, Europhys. Lett. **134**, 20007 (2021).
[37] Q. Li, J.-L. Ma, and L. Tan, Phys. Scr. **96**, 125709 (2021).
[38] F. Nissen, S. Schmidt, M. Biondi, G. Blatter, H. E. Türeci, and J. Keeling, Phys. Rev. Lett. **108**, 233603 (2012).
[39] M. Rigol, Phys. Rev. Lett. **103**, 100403 (2009).
[40] M. A. Cazalilla, R. Citro, T. Giamarchi, E. Orignac, and M. Rigol, Rev. Mod. Phys. **83**, 1405 (2011).
[41] L. Guo, S. Greschner, S. Zhu, and W. Zhang, Phys. Rev. A **100**, 033614 (2019).
[42] H. Wei, J. Zhang, S. Greschner, T. C. Scott, and W. Zhang, Phys. Rev. B **103**, 184501 (2021).
[43] M. R. Zirnbauer, J. Math. Phys. **62**, 021101 (2021).
[44] M. Brenes, T. LeBlond, J. Goold, and M. Rigol, Phys. Rev. Lett. **125**, 070605 (2020).
[45] A. Russomanno, M. Fava, and R. Fazio, Phys. Rev. B **102**, 144302 (2020).
[46] D. J. Luitz, N. Laflorencie, and F. Alet, Phys. Rev. B **91**, 081103(R) (2015).
[47] S. D. Geraedts, R. Nandkishore, and N. Regnault, Phys. Rev. B **93**, 174202 (2016).

[48] Y. Zhao, R. Narayanan, and J. Cho, Phys. Rev. B **102**, 094201 (2020).
[49] B. Bauer and C. Nayak, J. Stat. Mech.: Theory Exp. (2013) P09005.
[50] V. Khemani, S. P. Lim, D. N. Sheng, and D. A. Huse, Phys. Rev. X **7**, 021013 (2017).
[51] M. Žnidarič, T. Prosen, and P. Prelovšek, Phys. Rev. B **77**, 064426 (2008).
[52] J. H. Bardarson, F. Pollmann, and J. E. Moore, Phys. Rev. Lett. **109**, 017202 (2012).
[53] M. Serbyn, Z. Papić, and D. A. Abanin, Phys. Rev. Lett. **110**, 260601 (2013).
[54] D. N. Page, Phys. Rev. Lett. **71**, 1291 (1993).
[55] T. LeBlond, K. Mallayya, L. Vidmar, and M. Rigol, Phys. Rev. E **100**, 062134 (2019).